Available online at www.sciencedirect.com
ScienceDirect
Journal of Power Sources 162 (2006) 1067–1072
JOURNAL OF POWER SOURCES
www.elsevier.com/locate/jpowsour

Short communication

High performance rare earth oxides LnO_x (Ln = Sc, Y, La, Ce, Pr and Nd) modified Pt/C electrocatalysts for methanol electrooxidation

Zhicheng Tang, Gongxuan Lu *

State Key Laboratory for Oxo Synthesis and Selective Oxidation, Lanzhou Institute of Chemical Physics, Chinese Academy of Sciences and Graduate School of the Chinese Academy of Sciences, Lanzhou 730000, China

Received 18 June 2006; received in revised form 20 July 2006; accepted 20 July 2006
Available online 1 September 2006

Abstract

In this paper, the LnO_x (Ln = Sc, Y, La, Ce, Pr and Nd) modified Pt/C catalysts were prepared by wet precipitation and reduction method. The catalysts were characterized by transmission electron microscopy (TEM), energy dispersive X-ray analysis (EDX) and X-ray diffraction (XRD). TEM showed that the Pt-PrO_x nanoparticles were uniformly dispersed on carbon with an average particle size of 5.0 nm in the Pt_3-$(PrO_x)_1$/C catalyst. EDX showed that Pt and Pr were successfully loaded on the carbon support without obvious loss. XRD showed that all the Pt/C and LnO_x modified Pt/C electrocatalysts (except for the Pt_3-$(ScO_x)_1$/C electrocatalyst) displayed the typical character of Pt face centered cubic (fcc) phase, whereas the Pt_3-$(ScO_x)_1$/C electrocatalyst contained the diffraction pattern of Pt face centered cubic and Sc_2O_3 phase. LnO_x modified Pt/C electrocatalysts were compared with Pt/C in terms of the electrochemical activity and stability for methanol electrooxidation using cyclic voltammetry (CV) and chronoamperometry (CA) in 0.5 M H_2SO_4 + 0.5 M CH_3OH solutions. The results showed that all the LnO_x (except for NdO_x) modified the Pt/C electrocatalysts gave higher catalytic activity and stability than Pt/C. In particular, the Pt_3-$(PrO_x)_1$/C eloctrocatalyst was found to be superior than others. Under this respect, several Pt-PrO_x/C catalysts with different atomic ratio of Pt/Pr were also identically prepared and characterized. It was found by CV and CA that the Pt_3-$(PrO_x)_1$/C and Pt_1-$(PrO_x)_1$/C catalysts showed better catalytic activity and stability than the Pt_5-$(PrO_x)_1$/C, Pt_1-$(PrO_x)_3$/C and Pt/C catalysts. The Pt_3-$(PrO_x)_1$/C and Pt_1-$(PrO_x)_1$/C catalysts had high catalytic activity and good stability, which could be used as novel electrocatalysts for direct methanol fuel cell.

Keywords: Methanol electrooxidation; Direct methanol fuel cell; Rare earth oxides; Electrochemical properties; Electrocatalytic reaction; Electrocatalyst

1. Introduction

In the past decades, direct methanol fuel cells (DMFCs) have attracted extensive attention due to its advantages of low operating temperature (<100 °C), easy transportation and storage of fuel, high energy efficiency, low exhaustion and fast start-up of fuel [1–3]. However, two problems of the slow reaction of anode methanol oxidation at low temperature and the methanol crossover from anode to cathode are the main challenge for the commercialization of DMFCs [4]. Pt is the most active electrocatalyst for the oxidation of methanol, but intermediates species CO remain adsorbed on the surface and inhibit the oxidation reaction [5]. Therefore, Pt-based alloy or nanocomposite catalysts by alloying or mixing platinum with other elements need to be designed and synthesized. The CO poisoned platinum can be regenerated via the reaction of surface CO with oxygen species associated with an oxophilic elemental such as ruthenium to yield CO_2 [6]. High activity, stability and CO-tolerance of Pt-based electrocatalysts under acid environment are suitable for electrooxidation of many small chemicals molecular such as methanol. So it is necessary to prepare some effective anode catalysts satisfying with the properties mentioned above. In order to improve the activity of methanol electrooxidation, many catalysts such as PtRu, PtSn, PtRe and PtOs [7–10], and many preparation methods such as impregnation, colloid and microemulsion [11–13] have been applied.

In recent years, it is found that certain metal oxides, such as RuO_2 [14], WO_3 [15], ZrO_2 [16], MgO [17] and CeO_2 [18], can enhance the catalytic activity for ethanol or methanol electrooxidation through synergetic interaction with Pt. Among those, rare earth oxides exhibit a number of characteristics that make them interesting for catalytic studies. For example, ceria is a

* Corresponding author. Tel.: +86 931 4968178; fax: +86 931 4968178.
E-mail address: gxlu@lzb.ac.cn (G. Lu).

0378-7753/$ – see front matter © 2006 Elsevier B.V. All rights reserved.
doi:10.1016/j.jpowsour.2006.07.052

fluorite oxide, whose cation can switch between +3 and +4 oxidation states and ceria-based catalysts have been investigated for water–gas shift reactions [19]. Recently, ceria-based electrocatalysts have also been reported by Xu and Shen [18] and Cabrera and co-workers [20]. However, though these electrocatalysts show an improved performance according to the report of Xu and Shen [18], the reaction environment is alkaline, not acid media. In addition, other rare earth oxides may be have better performance than ceria, but have not been reported up to now. In this paper, we choose the wide-used rare earth oxides LnO_x (Ln = Sc, Y, La, Ce, Pr and Nd) as modifications to prepare the catalysts for methanol electrooxidation in acid electrolyte. The electrocatalytic activity and stability was evaluated using cyclic voltammetry (CV) and chronoamperometry (CA). The catalysts were characterized by means of XRD, TEM and EDX analysis.

2. Experimental details

2.1. Chemicals

All chemicals were analytically pure and used as received. The precursors of Y, La and Ce were their corresponding nitrates and the precursors of Sc and Pr were their corresponding oxides. The $NdCl_3$ and H_2PtCl_6 were used as precursors of Nd and Pt, respectively. All of the chemical reagents used in this article were purchased from Shanghai Chemical Reagents Corporation. Active carbon of Vulcan XC-72 with a BET area of about 240 $m^2\ g^{-1}$ (Cabot Corp.) was used as a carrier.

2.2. Catalyst preparation

Rare earth oxides modified Pt/C electrocatalysts, such as Pt-ScO_x/C, Pt-YO_x/C, Pt-LaO_x/C, Pt-CeO_x/C, Pt-PrO_x/C and Pt-NdO_x/C were prepared according to the report [16] with some modifications. First, Sc_2O_3 and Pr_2O_3 were dissolved in l.0 mL of concentrated HNO_3. Then the rare earth precursors were dissolved in 20 mL of mixture of distilled water and ethanol (v:v = 1:1) and mixed with 129.6 mg of carbon black (Vulcan XC-72). After ultrasonically mixed for 10 min, 2 mL of 0.02 M Na_2CO_3 aqueous solutions were then added into the mixture to form precipitates. The precipitates were washed with distilled water and dried in oven at 373 K for 10 h. The materials were finally calcinated at 600 °C for 2 h in Ar atmosphere to obtain LnO_x/C. Pt-LnO_x/C catalysts were prepared by reducing of H_2PtCl_6 with excessive $NaBH_4$ on LnO_x/C powders. The amount of H_2PtCl_6 was varied to control the molar ratio of Pt to LnO_x in the final catalysts. The nominal loading of Pt + LnO_x in the catalysts was 10%. All catalysts were marked as $Pt_m(LnO_x)_n$/C, where the subscript denoted the atomic ratio of Pt with LnO_x.

2.3. Physical characterization

The samples after reaction were transferred under a N_2 atmosphere to the diffractometer, and powder X-ray diffraction (XRD) patterns of the samples were recorded on a Rigakel B/Max-RB diffractometer with a nickel filtrated Cu Kα radiation. 2θ angles from 10° to 90° were recorded at a scanning speed of 2° min^{-1}.

Specimens were prepared for TEM analysis by ultrasonically suspending the catalyst powder in ethanol. A drop of suspension was then applied onto clean copper grids and dried in air. Samples were examined using the JEOL JEM-2010 electron microscope operated at 100 kV. The bulk composition of the as-prepared catalysts was evaluated by energy dispersive X-ray analysis (EDX) in a transmission electron microscopy.

2.4. Preparation of electrodes and electrochemical measurements

Electrochemical activities of catalysts were measured by cyclic voltammetry and chronoamperometry method using a standard three-electrode cell at the computer-controlled CHI660A electrochemical workstation. Five milligram of catalysts were suspended in 1.0 mL ethanol and 20 μL 10.0% Nafion was added as adhesive and proton conductor. The mixtures were ultrasonically scattered for 10 min to form homogeneous ink. Then, 20 μL ink was dropped on the glassy carbon (GC) electrode to act as the working electrode. A Pt wire and saturated calomel electrode (SCE) were used as the counter and reference electrode, respectively. Methanol oxidation experiment was measured in a solution of 0.5 M H_2SO_4 + 0.5 M CH_3OH at room temperature. For all experiments the sweep rate was 50 mV s^{-1}. The chronoamperometry curves were investigated in a solution of 0.5 M H_2SO_4 + 0.5 M CH_3OH at 0.65 V at room temperature. The unit of mA mg^{-1} used in the article was the theory loadings of Pt without accounts the actual loadings.

3. Results and discussion

The different diffractograms of various LnO_x modified Pt/C catalysts and Pt-PrO_x/C catalysts with different ratios are shown in Figs. 1 and 2. By examining the XRD patterns reported in Figs. 1 and 2, there are no obvious differences among those

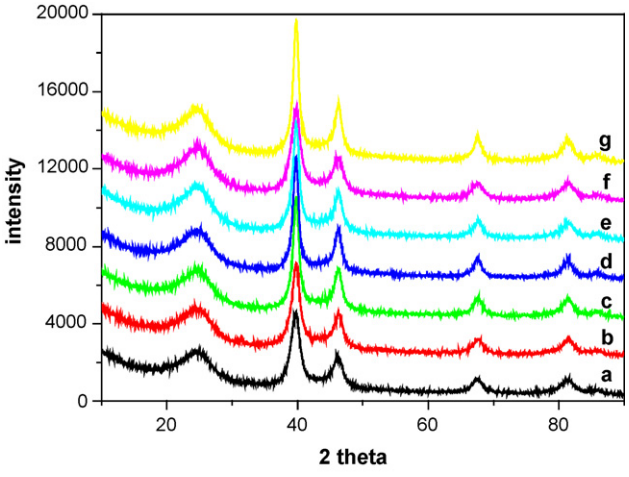

Fig. 1. X-ray diffraction patterns of the Pt/C and LnO_x modified Pt/C electrocatalysts. (a) Pt/C; (b) Pt_3-$(ScO_x)_1$/C; (c) Pt_3-$(YO_x)_1$/C; (d) Pt_3-$(LaO_x)_1$/C; (e) Pt_3-$(CeO_x)_1$/C; (f) Pt_3-$(PrO_x)_1$/C; (g) Pt_3-$(NdO_x)_1$/C.

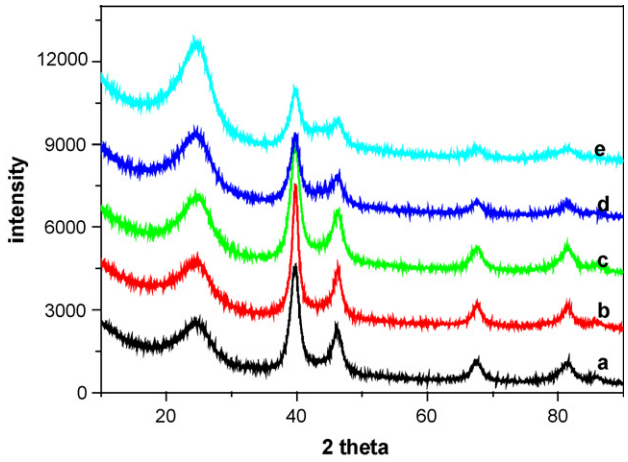

Fig. 2. X-ray diffraction patterns of the Pt/C and Pt-PrO_x/C electrocatalysts. (a) Pt/C; (b) Pt_5-$(PrO_x)_1$/C; (c) Pt_3-$(PrO_x)_1$/C; (d) Pt_1-$(PrO_x)_1$/C; (e) Pt_1-$(PrO_x)_3$/C.

Pt-LnO_x/C electrocatalysts. The diffraction peaks at 20–25° observed in all the XRD patterns of carbon-supported catalysts is due to the (0 0 2) phase of the hexagonal structure of Vulcan XC-72 carbon [21]. The diffraction peaks at about 39°, 46°, 68° and 81° are due to Pt(1 1 1), (2 0 0), (2 2 0) and (3 1 1) plane, respectively, which represents the typical character of Pt face centered cubic (fcc) phase [21]. There are no other distinct reflection peaks in all spectra than those of the peaks mentioned above except for the Pt_3-$(ScO_x)_1$/C electrocatalyst, indicating that all those catalysts have prevailed Pt (fcc) crystal structure. There are no character peaks of LnO_x, which indicated that LnO_x maybe have an amorphous structure. The diffractogram of the Pt_3-$(ScO_x)_1$/C electrocatalyst shows peaks at about $2\theta = 22°$, 31° and 52°, which are characteristic of Sc_2O_3 phase [22]. The reflections of Pt(2 2 0) are used to calculate the average particle size according the Scherrer formula [21]. The average particle size and lattice parameter obtained from XRD patterns and the TEM results are summarized in Table 1.

The average particle size of the Pt/C catalyst is found to be 7.1 nm, slightly lower than that of the Pt_3-$(ScO_x)_1$/C, Pt_3-$(YO_x)_1$/C, Pt_3-$(LaO_x)_1$/C and Pt_3-$(NdO_x)_1$/C catalysts, but larger than that of the Pt_3-$(CeO_x)_1$/C and all Pt-PrO_x/C catalysts. The average particle size decreases with the increase of PrO_x content in all the Pt-PrO_x/C catalysts. This suggests that the addition of PrO_x species can inhibit the agglomeration of Pt particles. The lattice parameter of the (fcc) Pt/C catalyst is estimated to be 3.915 Å and approaches the LnO_x modified Pt/C catalysts, showing that all the LnO_x modified Pt/C catalysts are non-alloy and LnO_x maybe exist as an amorphous structure. The average particle size and lattice parameter obtained from the XRD patterns are listed in Table 1.

Table 1
XRD and TEM results of the Pt/C and Pt-LnO_x/C electrocatalysts

Catalyst	Mean particle size (nm)		Lattice parameter (Å)
	TEM	XRD	
Pt/C	6.9	7.1	3.915
Pt_3-$(ScO_x)_1$/C	–	7.2	3.911
Pt_3-$(YO_x)_1$/C	–	7.4	3.912
Pt_3-$(LaO_x)_1$/C	–	7.2	3.917
Pt_3-$(CeO_x)_1$/C	6.5	6.6	3.912
Pt_3-$(NdO_x)_1$/C	–	7.5	3.918
Pt-PrO_x/C (Pt/Pr=)			
5:1	–	7.0	3.913
3:1	5.0	5.4	3.917
1:1	–	4.8	3.913
1:3	4.1	4.4	3.896

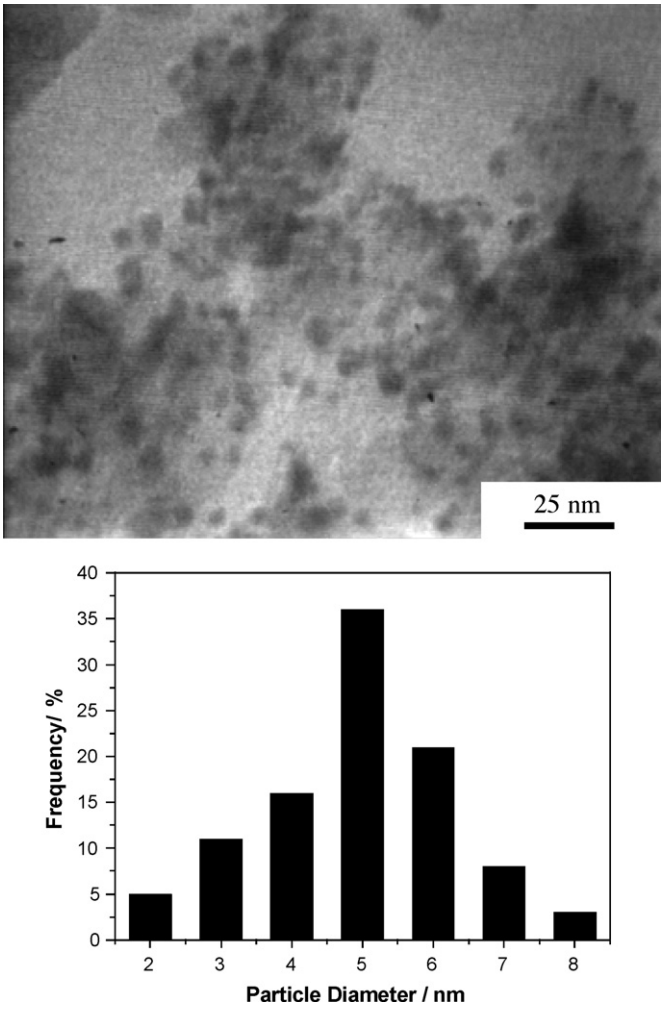

Fig. 3. TEM image and the corresponding size distribution of the Pt_3-$(PrO_x)_1$/C catalyst.

Fig. 3 shows the typical TEM image of the Pt_3-$(PrO_x)_1$/C catalyst and its particle size distribution. As can be seen from this figure, the platinum particles in the Pt_3-$(PrO_x)_1$/C catalyst are uniform and well distributed. Based on the measurements of 200 particles in random regions, the average particle size is estimated to be 5.0 nm for the Pt_3-$(PrO_x)_1$/C catalyst. The corresponding particle size distribution curve reveals that the particle size distribution is narrow. While for the Pt/C catalyst, the Pt nanoparticles on carbon are uniform in most regions but coalescent in others. The corresponding size distribution curve indicates a broad size distribution with an average size of 6.9 nm. The formation and dispersion of Pt nanoparticles on the carbon support may be due to the function of LnO_x. The average particle

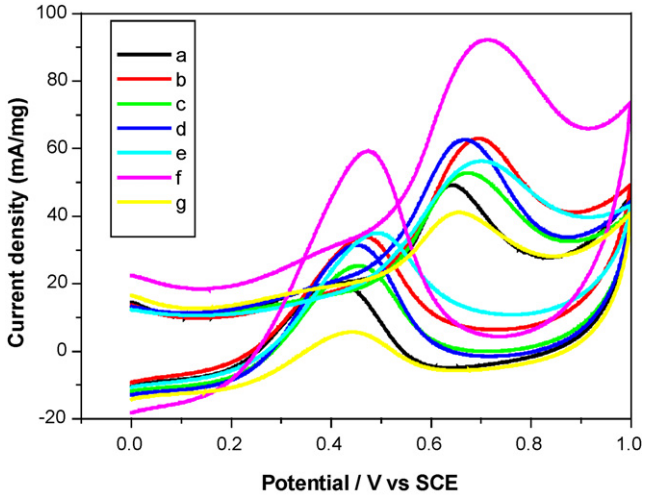

Fig. 4. Cyclic voltammograms of the Pt/C and LnO_x modified Pt/C electrocatalysts in the 0.5 M H_2SO_4 + 0.5 M CH_3OH solutions at a sweep rate of 50 mV s^{-1}. (a) Pt/C; (b), Pt_3-$(ScO_x)_1$/C; (c) Pt_3-$(YO_x)_1$/C; (d) Pt_3-$(LaO_x)_1$/C; (e) Pt_3-$(CeO_x)_1$/C; (f) Pt_3-$(PrO_x)_1$/C; (g) Pt_3-$(NdO_x)_1$/C.

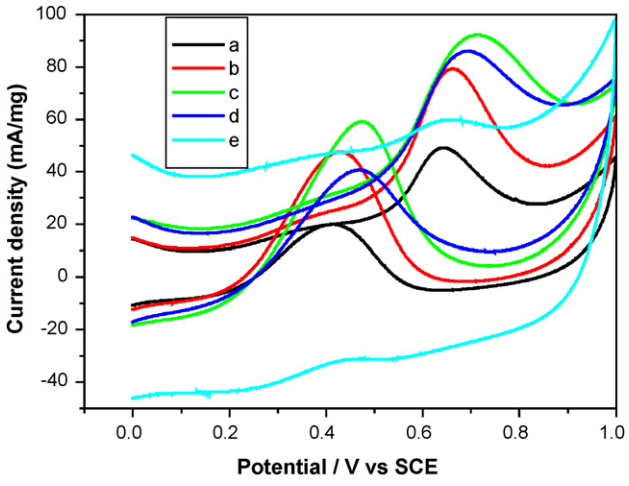

Fig. 5. Cyclic voltammograms of the Pt/C and Pt-PrO_x/C electrocatalysts in the 0.5 M H_2SO_4 + 0.5 M CH_3OH solutions at a sweep rate of 50 mV s^{-1}. (a) Pt/C; (b) Pt_5-$(PrO_x)_1$/C; (c) Pt_3-$(PrO_x)_1$/C; (d) Pt_1-$(PrO_x)_1$/C; (e) Pt_1-$(PrO_x)_3$/C.

size of the Pt_3-$(CeO_x)_1$/C and Pt_1-$(PrO_x)_3$/C catalysts is found to be 6.5 and 4.1 nm, and lower than that of Pt/C. The values of the average particle size obtained by TEM analysis are almost in good agreement with those calculated from the XRD results. EDX evaluation of the bulk composition of the Pt_3-$(PrO_x)_1$/C catalyst shows that the atomic ratios of Pt:Pr are 77:23, which is approximately same as those of the molar ratios of Pt to Pr in the solution. This results show that Pt and Pr are successfully loaded to the carbon support without obvious loss.

The cyclic voltammogram curves of the Pt_3-$(LnO_x)_1$/C catalysts in 0.5 M H_2SO_4 + 0.5 M CH_3OH solutions are shown in Fig. 4. The positive peak potential and corresponding peak current density of methanol electrooxidation are listed in Table 2. As can be seen from Fig. 4, there is no significant difference between the voltammograms of methanol oxidation on the Pt/C and Pt-LnO_x/C catalysts. Peaks appear in both the forward and reverse scans. In the forward scan the catalysts show a methanol oxidation peak at 0.66–0.71 V for all samples. Another peak is detected in the reverse scan, which is commonly attributed to the reactivation of oxidized platinum oxides. From Fig. 4 and Table 2, it is clear that the addition of rare earth oxides to Pt does not obviously change the peak potential of methanol electrooxidation. The peak potential of all the Pt/C and Pt-LnO_x/C catalysts ranges from 0.66 to 0.71 V. Except for the Pt_3-$(NdO_x)_1$/C catalyst, the current density at the first peak of methanol electrooxidation on the LnO_x modified Pt/C catalysts is higher than that on Pt/C (in this order: Pt_3-$(PrO_x)_1$/C > Pt_3-$(LaO_x)_1$/C ≈ Pt_3-$(ScO_x)_1$/C > Pt_3-$(CeO_x)_1$/C > Pt_3-$(YO_x)_1$/C > Pt/C > Pt_3-$(NdO_x)_1$/C). The current density at the positive peak on the Pt_3-$(CeO_x)_1$/C catalyst is higher than that on the Pt_3-$(YO_x)_1$/C, Pt/C and Pt_3-$(NdO_x)_1$/C catalysts, but less than that on the Pt_3-$(PrO_x)_1$/C, Pt_3-$(LaO_x)_1$/C and Pt_3-$(ScO_x)_1$/C catalysts. The Pt_3-$(PrO_x)_1$/C electrocatalyst shows the highest current density, but also has a slightly higher overpotential (0.71 V) than the Pt/C electrocatalyst. The Pt_3-$(LaO_x)_1$/C and Pt_3-$(ScO_x)_1$/C electrocatalysts have similar peak current density, but the former has a lower overpotential. The Pt_3-$(NdO_x)_1$/C catalyst shows the worst activity, and even lower than Pt/C catalyst, which may be due to the large particle size and bad dispersion. In the paper of Xu and Shen [18], the Pt-CeO_2/C catalyst shows a good electrocatalytic activity to alcohols (methanol, ethanol, glycerol and EG) in alkaline media. However, the Pt-CeO_2/C catalyst does not show special excellent electrocatalytic activity to methanol in acid media as reported in our paper. Oppositely, it is clear that the Pt_3-$(PrO_x)_1$/C catalyst presents the highest positive peak current density, and consequently highest activity to methanol electrooxidation from the point of current density. The Pt_3-$(LaO_x)_1$/C and Pt_3-$(ScO_x)_1$/C electrocatalysts also show higher activity to methanol electrooxidation among all electrocatalysts, which indicates that the Pt_3-$(LaO_x)_1$/C and Pt_3-$(ScO_x)_1$/C catalysts are also promising catalysts for methanol electrooxidation.

Table 2
CV results of the Pt/C and Pt-PrO_x/C electrocatalysts

Catalysts	Positive peak potential (V vs. SCE)	Peak current density (mA mg^{-1})
Pt/C	0.66	49.1
Pt_3-$(ScO_x)_1$/C	0.69	62.9
Pt_3-$(YO_x)_1$/C	0.67	52.7
Pt_3-$(LaO_x)_1$/C	0.66	62.6
Pt_3-$(CeO_x)_1$/C	0.70	56.3
Pt_3-$(NdO_x)_1$/C	0.66	40.9
Pt_5-$(PrO_x)_1$/C	0.67	79.1
Pt_3-$(PrO_x)_1$/C	0.71	92.2
Pt_1-$(PrO_x)_1$/C	0.70	86.0
Pt_1-$(PrO_x)_3$/C	0.66	59.7

The cyclic voltammogram curves of the Pt/C and Pt-PrO_x/C catalysts with different atomic ratios of Pt/Pr (Pt/Pr = 5/1, 3/1, 1/1, 1/3) are shown in Fig. 5. The scan rate is 50 mV s^{-1} in the potential range of 0.0–1.0 V versus SCE in 0.5 M H_2SO_4 + 0.5 M CH_3OH solutions. The cyclic voltammogram of methanol oxi-

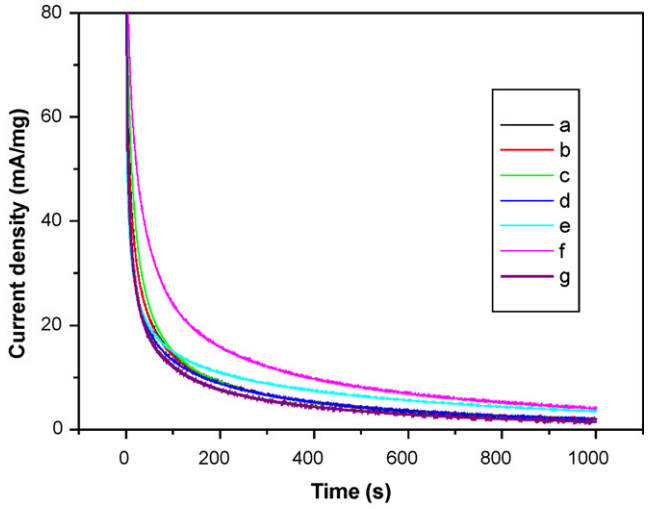

Fig. 6. Chronoamperometry of the Pt/C and LnO_x modified Pt/C electrocatalysts in the 0.5 M H_2SO_4 + 0.5 M CH_3OH solutions at 0.65 V vs. SCE. (a) Pt/C; (b) Pt_3-$(ScO_x)_1$/C; (c) Pt_3-$(YO_x)_1$/C; (d) Pt_3-$(LaO_x)_1$/C; (e) Pt_3-$(CeO_x)_1$/C; (f) Pt_3-$(PrO_x)_1$/C; (g) Pt_3-$(NdO_x)_1$/C.

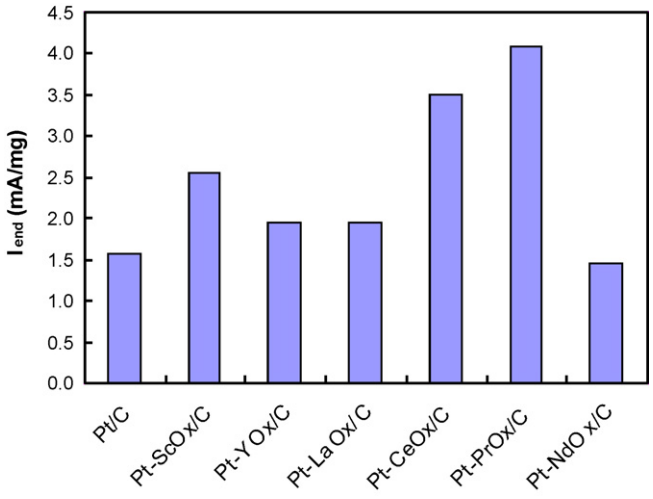

Fig. 7. Current density values at 1000 s during chronoamperometry experiments for the Pt/C and Pt-LnO_x/C catalysts.

dation shows similar feature on the PrO_x modified Pt/C electrocatalysts except for the Pt_1-$(PrO_x)_3$/C catalyst. The peak current density of methanol oxidation increases as the increase of PrO_x content in the catalysts (Pt_5-$(PrO_x)_1$/C and Pt_3-$(PrO_x)_1$/C), and then decreases (Pt_1-$(PrO_x)_1$/C and Pt_1-$(PrO_x)_3$/C). The current density of the Pt/C catalyst is lower than that of the Pt_3-$(PrO_x)_1$/C, Pt_1-$(PrO_x)_1$/C and Pt_5-$(PrO_x)_1$/C catalysts, but higher than that of the Pt_1-$(PrO_x)_3$/C catalyst if the current of the double layer is subtracted. The Pt_1-$(PrO_x)_3$/C catalyst is a relatively inactive catalyst toward methanol oxidation. The Pt_3-$(PrO_x)_1$/C and Pt_1-$(PrO_x)_1$/C catalysts show higher peak current density, indicating that these two catalysts are ideal electrocatalysts for methanol electrooxidation.

To measure the electrochemical stability of the LnO_x modified Pt/C catalysts for methanol oxidation, chronoamperometry experiments are carried out. Fig. 6 presents the CA curves obtained in 0.5 M H_2SO_4 + 0.5 M CH_3OH solutions at an anodic potential of 0.65 V versus SCE. This potential is chosen because it is close to the positive peak potential of methanol electrooxidation in the cyclic voltammogram curves. In all of the CA curves there is a sharp initial current drop in the first 300 s, and follows by a slower decay. Representative chronoamperograms obtained at 0.65 V for different electrodes are shown in Fig. 6. The final current density values at 1000 s during chronoamperommetric experiments are presented in Fig. 7. In long runs it is found that the current density obtained on the Pt_3-$(PrO_x)_1$/C catalyst is higher than that on others. The final current density after holding the cell potential at 0.65 V versus SCE for 1000 s are following: Pt_3-$(PrO_x)_1$/C > Pt_3-$(CeO_x)_1$/C > Pt_3-$(ScO_x)_1$/C > Pt_3-$(LaO_x)_1$/C > Pt_3-$(YO_x)_1$/C > Pt/C > Pt_3-$(NdO_x)_1$/C. The result is nearly consistent with the CV results. The Pt_1-$(CeO_x)_1$/C electrocatalyst shows a higher stability than the Pt_3-$(ScO_x)_1$/C and Pt_3-$(LaO_x)_1$/C electrocatalysts, though the former has lower activity. The Pt_3-$(PrO_x)_1$/C electrocatalyst has the highest current density (4.09 mA mg^{-1}), which is far larger (2.6 times) than that of the Pt/C (1.56 mA mg^{-1}) electrocatalyst. The test shows that the Pt_3-$(PrO_x)_1$/C electrocatalyst has the best electrocatalytic performance among all the Pt/C and LnO_x modified Pt/C electrocatalysts.

The Pt/C and Pt-PrO_x/C electrocatalysts with different ratio of Pt/Pr are biased at 0.65 V versus SCE in 0.5 M H_2SO_4 + 0.5 M CH_3OH solutions and the changes in their current density with time are recorded in Fig. 8. The final current density values at 1000 s during CA experiments are presented in Fig. 9 for all the Pt/C and Pt-PrO_x/C electrocatalysts. For all the Pt/C and Pt-PrO_x/C electrocatalysts, a pronounced decay of the current density is observed at the beginning of the curves. During the first 300s, the current decreases quickly, and slow to evolve toward a steady state value in the following 700s of the experiment. The final current density of different electrocatalysts increases in the order: Pt_1-$(PrO_x)_3$/C < Pt_5-$(PrO_x)_1$/C < Pt_3-$(PrO_x)_1$/C ≈ Pt_1-$(PrO_x)_1$/C. The final current density of the Pt_3-$(PrO_x)_1$/C and Pt_1-$(PrO_x)_1$/C electrocatalysts

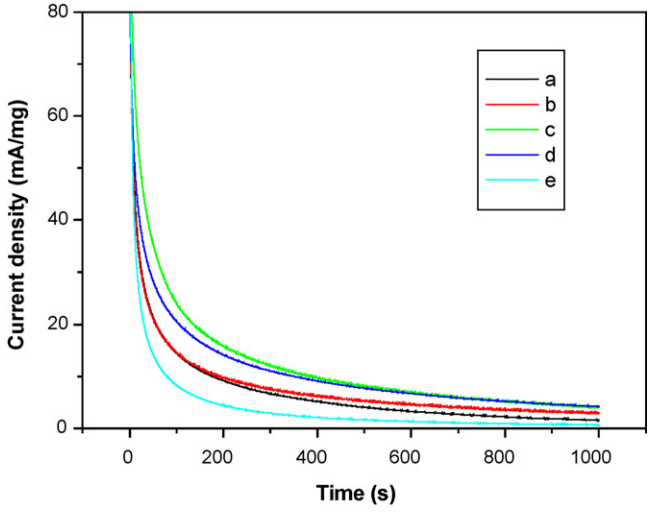

Fig. 8. Chronoamperometry of the Pt/C and Pt-PrO_x/C electrocatalysts in the 0.5 M H_2SO_4 + 0.5 M CH_3OH solutions at 0.65 V vs. SCE. (a) Pt/C; (b) Pt_5-$(PrO_x)_1$/C; (c) Pt_3-$(PrO_x)_1$/C; (d) Pt_1-$(PrO_x)_1$/C; (e) Pt_i-$(PrO_x)_3$/C.

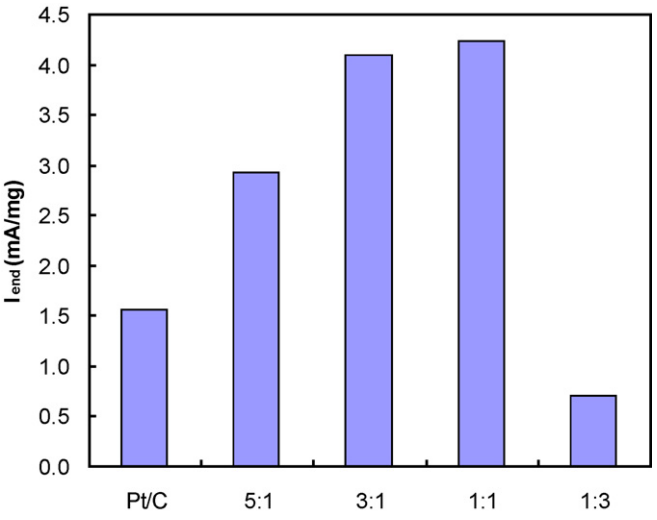

Fig. 9. Current density values at 1000 s during chronoamperometry experiments for the Pt/C and Pt-PrO_x/C with different atomic ratios of Pt/Pr = 5/1, 3/1, 1/1 and 1/3.

are similar, and higher than others, which indicates that the two catalysts have good stability and activity.

Cyclic voltammogram and chronoamperometry show that LnO_x (Ln = Sc, Y, La, Ce, Pr) can use as modifications to improve the electrocatalytic activity of the Pt/C electrocatalyst for methanol electrooxidation. In particular, the Pt_3-$(PrO_x)_1$/C and Pt_1-$(PrO_x)_1$/C electrocatalysts have excellent electrocatalytic activity and good stability toward methanol electrooxidation, which may be attributed to the small particle size and high dispersion of Pt and PrO_x. LnO_x can supply surface oxygen-containing species for the oxidative removal of CO-like species strongly adsorbed on adjacent active sites [23]. The LnO_x modified Pt/C catalysts improve the removal of CO_{ads} species formed on the platinum surface during methanol electrooxidation. Therefore, the addition of LnO_x to Pt enhances the electrooxidation activity of methanol. Pt active sites of catalysts with a too high PrO_x content can be partly blocked by surface Pr oxides, which will inhibit methanol adsorption and oxidation. The chemisorbed CO-like intermediate cannot be completely removed when the PrO_x content in the catalysts is too low. Therefore, it is reasonable that LnO_x can improve the electrocatalytic activity for methanol electrooxidation, and the Pt_3-$(PrO_x)_1$/C and Pt_1-$(PrO_x)_1$/C electrocatalysts have the highest activity and best stability.

4. Conclusion

LnO_x (Ln = Sc, Y, La, Ce, Pr and Nd) promoted Pt/C electrocatalysts were prepared by wet precipitation and reduction method. The preliminary results indicated that the addition of LnO_x (except for NdO_x) into Pt/C catalysts could significantly improve the electrode performance for methanol oxidation in this order: Pt_3-$(PrO_x)_1$/C > Pt_3-$(LaO_x)_1$/C ≈ Pt_3-$(ScO_x)_1$/C > Pt_3-$(CeO_x)_1$/C > Pt_3-$(YO_x)_1$/C > Pt/C > Pt_3-$(NdO_x)_1$/C. The Pt_3-$(PrO_x)_1$/C catalyst had the best results. The Pt-PrO_x/C catalysts with different ratios of Pt/Pr were also prepared and characterized by XRD, TEM, EDX, CV and CA. The final results showed that the Pt_3-$(PrO_x)_1$/C and Pt_1-$(PrO_x)_1$/C electrocatalysts had the highest activity and best stability than others. The better performance could attribute to the so-called bifunctional mechanism and the electronic interaction between Pt and LnO_x. The Pt_3-$(PrO_x)_1$/C and Pt_1-$(PrO_x)_1$/C electrocatalysts having good synergetic effect, supplying sufficient $-OH_{ads}$ and eliminating $-CO_{ads}$ poisoning, were the appropriate anode catalyst for direct methanol fuel cell.

References

[1] C. Lamy, A. Lima, V. LeRhun, F. Delime, C. Coutanceau, J.M. Léger, J. Power Sources 105 (2002) 283–296.
[2] T. Iwasita, Electrochim. Acta 47 (2002) 3663–3674.
[3] A. Hamnett, Catal. Today 38 (1997) 445–457.
[4] H. Liu, C. Song, L. Zhang, J. Zhang, H. Wang, D.P. Wilkinson, J. Power Sources 155 (2006) 95–110.
[5] M.B. de Oliveira, L.P.R. Profeti, P. Olivi, Electrochem. Commun. 7 (2005) 703–709.
[6] Q. Lu, B. Yang, L. Zhuang, J. Lu, J. Phys. Chem. B 109 (2005) 1715–1722.
[7] J. Guo, G. Sun, Q. Wang, G. Wang, Z. Zhou, S. Tang, L. Jiang, B. Zhou, Q. Xin, Carbon 44 (2006) 152–157.
[8] L. Jiang, G. Sun, S. Sun, J. Liu, S. Tang, H. Li, B. Zhou, Q. Xin, Electrochim. Acta 50 (2005) 5384–5389.
[9] K.B. Kokoh, F. Hahn, E.M. Belgsir, C. Lamy, A.R. de Andrade, P. Olivi, A.J. Motheo, G. Tremiliosi-Filho, Electrochim. Acta 49 (2004) 2077–2083.
[10] B.N. Grgur, N.M. Markovic, P.N. Ross, Electrochim. Acta 43 (1998) 3631–3635.
[11] B. Yang, Q. Lu, Y. Wang, L. Zhuang, J. Lu, P. Liu, J. Wang, R. Wang, Chem. Mater. 15 (2003) 3552–3557.
[12] Z. Tang, D. Geng, G. Lu, J. Colloid Interf. Sci. 287 (2005) 159–166.
[13] X. Zhang, K.-Y. Chan, Chem. Mater. 15 (2003) 451–459.
[14] H.M. Villullas, F.I. Mattos-Costa, L.O.S. Bulhoes, J. Phys. Chem. B 108 (2004) 12898–12903.
[15] J. Shim, C. Lee, H. Lee, J. Lee, E.J. Cairns, J. Power Sources 102 (2001) 172–177.
[16] Y. Bai, J. Wu, J. Xi, J. Wang, W. Zhu, L. Chen, X. Qiu, Electrochem. Commun. 7 (2005) 1087–1090.
[17] C. Xu, P.K. Shen, X. Ji, R. Zeng, Y. Liu, Electrochem. Commun. 7 (2005) 1305–1308.
[18] C. Xu, P.K. Shen, Chem. Commun. 19 (2004) 2238–2239.
[19] Q. Fu, H. Saltsburg, M. Flytzani-Stephanopoulos, Science 301 (2003) 935–938.
[20] C.L. Campos, C. Roldan, M. Aponte, Y. Ishikawa, C.R. Cabrera, J. Electroanal. Chem. 581 (2005) 206–215.
[21] Z.B. Wang, G.P. Yin, J. Zhang, Y.C. Sun, P.F. Shi, J. Power Sources, in press.
[22] T. Masui, Y.W. Kim, N. Imanaka, G. Adachi, J. Alloys Compd. 374 (2004) 97–100.
[23] C. Xu, R. Zeng, P.K. Shen, Z. Wei, Electrochim. Acta 51 (2005) 1031–1035.